Pisano, J. J., Prado, E., & Freedman, J. (1966) *Arch. Biochem. Biophys. 117*, 394-399.
Schiltz, E., Schnackerz, K. D., & Gracy, R. W. (1977) *Anal. Biochem. 79*, 33-41.
Taylor, S., & Tappel, A. L. (1973) *Anal. Biochem. 56*, 140-148.
Watterson, D. M., Burgess, W. H., Lukas, T. J., Iverson, D., Marshak, D. R., Schleicher, M., Erickson, B. W., Fok, K.-F., & Van Eldik, L. J. (1984) *Adv. Cyclic Nucleotide Protein Phosphorylation Res. 16*, 205-226.
Yuan, P. M., Talent, J. M., & Gracy, R. W. (1981) *Mech. Ageing Dev. 35*, 151-162.

Fluorescence Quenching in Model Membranes: Phospholipid Acyl Chain Distributions around Small Fluorophores†

Mark D. Yeager‡ and Gerald W. Feigenson*
Section of Biochemistry, Molecular and Cell Biology, Cornell University, Ithaca, New York 14853
Received August 7, 1989; Revised Manuscript Received December 20, 1989

ABSTRACT: Fluorescence quenching in lipid bilayers is treated by a new approach based on calculation of the probability distribution of quenching and nonquenching acyl chains around a fluorophore. The effect of acyl lattice site dependence (i.e., correlations of phospholipid sister chain occupancy of neighbor sites) was modeled by use of Monte Carlo simulations of acyl chain occupancy. This explicit accounting of site occupancy correlation was found to fit observed quenching behavior better than did a model wherein phospholipid quenchers are considered to be independent. A key aspect of this approach is to evaluate the rate for quenching in a bilayer composed of pure quenching lipid. In order to evaluate this quenching rate, and also to provide a strong test of the calculated probability distributions, we synthesized lipids with both acyl chains labeled with a quenching moiety (Br or nitroxide), as well as the more usual single-chain quenchers. The fluorescence of tryptophan octyl ester (TOE), and of the 1,6-diphenyl-1,3,5-hexatriene (DPH) derivatives trimethylammonium-DPH (TMA-DPH) and 1-lauroyl-2-(DPH-propionyl)phosphatidylcholine (DPH-PC), was examined. We obtained consistent results with all the fluorophores and quenchers indicating that up to 18 neighboring acyl sites can contribute to quenching, corresponding to two shells of acyl sites on a hexagonal lattice. Calculated *discrete* distributions of fluorescence intensities were converted into fluorescence lifetimes and compared with Gaussian and Lorentzian *continuous* lifetime distributions. The fluorescence quenching theory presented here may be used to explain quantitatively the heterogeneity of fluorophore environments in multicomponent membranes.

Fluorescence quenching has been a useful technique for investigating the structure and dynamics of the environment of membrane-bound fluorophores. Quenchers of various sizes, charges, and hydrophobic character have quantitatively different effects on fluorescent membrane components. For example, the "depth" at which a fluorophore resides in the membrane, relative to the aqueous interface, can be inferred from its accessibility to different quenchers (Chattopadhyay & London, 1987; Thulborn & Sawyer, 1978). By varying the location of a quencher in the hydrophobic region of the membrane, a low-resolution map of intrinsically fluorescent tryptophans of a membrane-embedded polypeptide can be established, if the primary sequence is known (Markello et al., 1985). Relative lipid-protein binding constants can be determined with phospholipid analogues of quenchers (Caffrey & Feigenson, 1981; East & Lee, 1982; London & Feigenson, 1981b). Quenching behavior can also be influenced by partitioning of a fluorophore between phases giving different quantum yield, as occurs with lateral separations of gel and fluid phases in binary mixtures induced by temperature or ion binding (Feigenson, 1983; Florine-Casteel & Feigenson, 1988; Huang et al., 1988; Lentz et al., 1976; London & Feigenson, 1981c; Sklar et al., 1979; Yguerabide & Foster, 1981). In the absence of lateral phase separations, for membrane-bound proteins with intrinsically fluorescent tryptophans, the location and degree of exposure of tryptophan residues relative to the quencher determines the observed fluorescent intensity. Quenching of intrinsic tryptophanyl fluorescence has been investigated with brominated lipids (Berkhout et al., 1987; East & Lee, 1982; Leto et al., 1980) and nitroxide-labeled lipids (Bieri & Wallach, 1975; Caffrey & Feigenson, 1981; Haigh et al., 1979; London & Feigenson, 1978).

Fluorescence quenching, except for resonance energy transfer, requires close approach of the fluorophore and quencher. Significant reductions of fluorescence intensity are usually interpreted according to theories of either dynamic or static quenching, or a combination of both (Lakowicz, 1983). These theories have been applied successfully to a wide variety of quenching studies in isotropic, low-viscosity solutions, including the determination of tryptophan side-chain exposure in soluble proteins (Eftink & Ghiron, 1976; Lehrer, 1971) and the quenching of small organic fluorophores in organic solvents (Atik & Singer, 1978; Green et al., 1973).

The proper treatment of membrane-bound fluorophores and quenchers requires additional considerations. The membrane is an anisotropic medium where lipid components are constrained to two dimensions and diffuse at much lower rates than in nonviscous solvents. The composition of a model membrane can be manipulated to consist *entirely* of a quenching phospholipid analogue, thereby achieving effective

† This work was supported by a grant from the National Institutes of Health, U.S. Public Health Service (HL-18255). M.Y. was supported in part by National Institutes of Health Research Service Award 5T32GM07273.
‡ Present address: Department of Biochemistry, Sciences II, University of Geneva, Ch-1211 Geneva 4, Switzerland.

0006-2960/90/0429-4380$02.50/0

quencher concentrations usually unattainable in solution studies. Such a model system has been treated in some detail by London and Feigenson (1981a, 1981b) using several small organic fluorophores, the polypeptide gramicidin, and the intrinsic membrane protein Ca^{2+}-ATPase. Two explicit features of this treatment are as follows: (1) a small fluorophore will not fluoresce if a single nearest neighbor is a quencher, which is the static quenching paradigm; (2) residual fluorescence in a membrane composed entirely of quenching lipid is considered to come from a completely "inaccessible" pool of fluorophores, which is reasonable for a large protein with many tryptophans. Also implicit in this quenching theory is the picture of the lateral structure of the membrane as a lattice of phospholipid sites rather than a lattice of acyl chains.

The theory of London and Feigenson, however, does not account for the cases of residual fluorescence at high quencher concentrations, caused simply by inefficient quenching. In particular, the theory does not yield physically appropriate values for the number of nearest neighbors of a fluorophore that is small and capable of intimate contact with the quenching groups, if there is significant residual fluorescence when the membrane is composed entirely of quenching lipid. As long as such a fluorophore is incorporated completely into the membrane then there should be no pools of inaccessible fluorescence. Brominated phospholipid quenching of tryptophan (this study), and spin-labeled phospholipid quenching of rhodamine PE[1] and R18 (Florine, Ye, and Feigenson, unpublished data) and indocarbocyanine probes (Spink et al., 1990) have all shown this inefficiency of quenching.

Theories of dynamic and static quenching depend on the assumption of bimolecular encounters between the fluorophore and quencher. A better description of quenching in membranes over the entire range of quencher concentrations must be able to handle the high probability of multiple, simultaneous encounters of many quenchers with one fluorophore. In this study, we derive a general theory to describe the fluorescence of small amphipathic fluorophores at all concentrations of quenching lipid. The theory accommodates different efficiencies of quenching and the presence of quenchers on one or both acyl chains of the quenching phospholipid. Monte Carlo simulations of lattice occupancy are used to calculate the probability densities of different fluorophore environments. These theoretical distributions of fluorophore environments are transformed into distributions of fluorescence lifetimes and compared to the continuous distributions used to analyze fluorescence lifetimes in membranes. We suggest that our steady-state quenching theory may be used to explain the heterogeneity of fluorophore environments and lifetimes seen in multicomponent membranes.

Experimental Procedures

Materials. Palmitoyloleoylphosphatidylcholine (POPC), dioleoylphosphatidylcholine (DOPC), and monolauroyllysophosphatidylcholine (lyso-PC) were from Avanti Polar Lipids, Inc. (Birmingham, AL). DL-Tryptophan octyl ester (TOE) and glycerophosphorylcholine (GPC-$CdCl_2$) were obtained from Sigma. CDI, DBU, and 7-doxylstearic acid were from Aldrich Chemical Co. (Milwaukee, WI). DPH-propionic acid and TMA-DPA were obtained from Molecular Probes (Junction City, OR). Silicic acid (Biosil A) was from BioRad. Pipes buffer (puriss grade) was from Fluka (Hauppauge, NY). Bromine was analytical grade from Mallinkrodt. Water was purified on a Milli-Q system (Millipore Corp., Bedford, MA). All organic solvents were HPLC grade; other inorganic chemicals were of reagent grade or better. All fluorophores were used without further purification.

SpinPC (also termed 8-PC) was synthesized by acylation of the 2 position of egg lyso-PC with an 8-doxylpalmitic acid derivative, as described previously (London & Feigenson, 1981a).

Methods. All purchased lipids used were judged >98% pure by TLC of 50–100 μg of lipid on Adsorbosil Plus P plates (Applied Science, State College, PA), prerun in chloroform/methanol (9:1, v/v), activated, loaded with lipid and developed with chloroform/methanol/ammonium hydroxide (28%) (65:35:6, v/v) or chloroform/methanol/water (65:25:3, v/v) and then visualized with Zinzadze spray and charring (Kates, 1986). Concentrations of stock phospholipids were determined by phosphate assay, as described previously (Kingsley & Feigenson, 1979). Fluorophore stocks were prepared as dilute chloroform (DPH) or methanol (TMA-DPH, TOE) solutions and stored at −80 °C. Concentrations were determined from weight measurements for TOE, and from absorbance measurements for TMA-DPH, $\epsilon_{361} = 70\,500$.[2]

Brominated Phosphatidylcholine Synthesis. Brominated PCs were synthesized from POPC and DOPC as previously described (Dawidowicz & Rothman, 1976; East & Lee, 1982), with some modifications. Solutions were cooled on crushed dry ice, and then 100 mg of lipid in chloroform (30 mM) was titrated with bromine in chloroform (300 mM). The bromine solution was added dropwise until a slight excess was present, indicated by the color of unreacted bromine. The reaction mixture was then loaded on a 10-g column of activated silicic acid packed in chloroform. Bromine was eluted with 10% methanol/chloroform, and the lipid was then eluted with 50% methanol/chloroform, as previously described (East & Lee, 1982). Phosphate-positive lipid fractions were checked by TLC and the acceptable fractions pooled and washed in a chloroform/methanol/water system, the aqueous phase composed of 100 mM EDTA, 100 mM NaCl, 50 mM Tris, pH 8.2 (Bligh & Dyer, 1959). The chloroform layer was collected, rotovapped to near dryness, and then washed again with 10 mM NaCl.

DPH-PC and Di-SpinPC Synthesis. DPH-PC (phosphatidylcholine labeled in the *sn*-2 position with DPH-propionic acid) and di-SpinPC were synthesized by a modification of

[1] Abbreviations: 8-doxylpalmitic acid, 2-(6-carboxyhexyl)-2-octyl-4,4-dimethyloxazolidinyl-3-oxy; 7-doxylstearic acid, 2-(5-carboxypentyl)-2-undecyl-4,4-dimethyloxazolidinyl-3-oxy; 8-PC, 1-acyl-2-[8-doxylpalmitoyl]-*sn*-glycero-3-phosphocholine; BrPC, 1-palmitoyl-2-(9,10-dibromostearoyl)-*sn*-glycero-3-phosphocholine; di-BrPC, 1,2-bis-(9,10-dibromostearoyl)-*sn*-glycero-3-phosphocholine; CDI, carbonyldiimidazole; DBU, 1,8-diazabicyclo[5.4.0]undec-7-ene; DOPC, 1,2-dioleoyl-*sn*-glycero-3-phosphocholine; DPH, 1,6-diphenyl-1,3,5-hexatriene; DPH-PC, 1-lauroyl-2-[[2-[4-(6-phenyl-*trans*-1,3,5-hexatrienyl)-phenyl]ethyl]carbonyl]-*sn*-glycero-3-phosphocholine; EDTA, ethylenediaminetetraacetic acid; F_0, fluorescence with 0 neighboring quenchers; F_M, fluorescence with M neighboring quenchers; FWHM, full-width at half-maximum; lyso-PC, 1-acyl-*sn*-glycero-3-phosphocholine; M, maximum number of interacting neighbor sites; PC, 1,2-diacyl-*sn*-glycero-3-phosphocholine; PE, 1,2-diacyl-*sn*-glycero-3-phosphoethanolamine; Pipes, piperazine-*N*,*N*′-bis(2-ethanesulfonic acid); POPC, 1-palmitoyl-2-oleoyl-*sn*-glycero-3-phosphocholine; POPS, 1-palmitoyl-2-oleoyl-*sn*-glycero-3-phosphoserine; R18, octadecylrhodamine B, chloride salt; SpinPC, 1-acyl-2-[8-doxylpalmitoyl]-*sn*-glycero-3-phosphocholine; di-SpinPC, 1,2-bis[7-doxylstearoyl]-*sn*-glycero-3-phosphocholine; τ_0, fluorescence lifetime in the absence of quencher; TMA-DPH, trimethylammonium-DPH.

[2] The extinction coefficient for TMA-DPH reported as 30 200 in dimethylformamide (Prendergast et al., 1981) is probably incorrect; the correct value in methanol is 70 500 (technical assistance, Molecular Probes, Inc., personal communication). An earlier report gave $\epsilon_{max} = 53\,000$ in methanol (Cundall et al., 1979). We obtained $\epsilon_{361} = 71\,600$ in methanol, in agremeent with Molecular Probes, Inc.

a method based on the condensation of an imidazolide activated fatty acid with lyso-PC [Boss et al. (1975); G. W. Feigenson, unpublished data]. For the synthesis of DPH-PC, DPH-propionic acid was dissolved in THF (0.1 mmol in 1.7 mL) with 0.1 mmol of CDI and allowed to form the imidazolide adduct for 1 h. The solution was then added to a DMF solution of lysolauroyl-PC (0.1 mmol in 2.5 mL) with DBU as a catalyst (Ohta et al., 1982; Staab, 1962). The reaction was stirred for 18 h at 45 °C. Products were purified on a medium-pressure column of Biosil A, 200–400 mesh, achieving separation of the lyso-PC from the PC product with $CHCl_3/MeOH/H_2O$ (65:25:3, v/v).

Phosphatidylcholine labeled in both the *sn*-1 and *sn*-2 position with 7-doxylstearic acid (di-SpinPC) was prepared in a manner similar to DPH-PC, but starting from GPC-$CdCl_2$ and the imidazolide of 7-doxylstearic acid. Fatty acid (0.06 mmol) was reacted with CDI in 0.3 mL of benzene for 1 h, and then added to 0.03 mmol of GPC-$CdCl_2$ in 0.6 mL of DMSO with DBU as catalyst. The reaction was stirred at 45 °C overnight, and the products were purified as for DPH-PC.

Sample Preparation. Multilammellar lipid vesicles were prepared in disposable 10 × 75 mm borosilicate culture tubes from stock chloroform solutions of phospholipid and fluorophore with a total of 0.2–0.5 μmol. Fluorophore to lipid ratios were 1:500 for DPH-PC and TMA-DPH and 1:150 for TOE. Solvent was evaporated under a stream of nitrogen. Samples were then dissolved in 50 μL of methanol/benzene (5:95, v/v), shelled, frozen in liquid nitrogen, and then lyophilized for 12–18 h. The methanol was necessary to solubilize the TOE, but did not depress the freezing point of the benzene solution enough to prevent lyophilization. Buffer (10 mM Pipes, 100 mM KCl, pH 7.0) was added to give a final lipid concentration of 1 mM. Samples were flushed with argon, sealed, and allowed to hydrate at room temperature for 2 h in the dark, followed by 10 s of vortex mixing to yield a suspension of multilayers. Fluorophore-free blanks were prepared identically for each lipid composition. Fluorescence values are expressed as the mean of three to five determinations and the standard deviation.

Incorporation of fluorophores into the multilayers was verified by centrifuging the lipid dispersions at 22000*g* for 45 min and checking the supernatant for residual fluorescence, which was negligible for all fluorophores and lipid compositions.

Fluorescence Spectroscopy. Fluorescence intensities were measured with a spectrofluorometer modified from initial descriptions (Caffrey & Feigenson, 1981) to extend the accuracy and reproducibility over the 2 orders of magnitude required for highly quenched samples. All measurements were conducted in photon counting mode using a pulse and current amplifier (Pacific Precision Instruments, Concord, CA) and a photomultiplier tube selected for low dark current (Thorn EMI 9789QA). Excitation/emission wavelengths (nm) for DPH-PC and TMA-DPH were 360/430; for TOE, 285/340. Bandwidths for the double monochromaters were 2 nm for excitation and 16 nm for emission. The 1 mM lipid samples were diluted into a 1 × 1 cm quartz cuvette to a final concentration of 100 μM in 1.5 mL total volume. Light scattering contribution to the measured fluorescence was insignificant at this lipid concentration. All measurements were made at 22 °C.

EPR Spectroscopy. EPR spectra were collected on a Varian E-4 X-band spectrometer, 100-kHz field modulation, interfaced to a DEC PDP-11/23 computer. Instrument settings were as previously described (Florine & Feigenson, 1987).

NMR Spectroscopy. ^1H NMR spectra were obtained on a Varian XL-200 spectrometer operating at 200 MHz.

Computations. All computations were performed on a Digital Equipment Corp. LSI 11/73 running the TSX-Plus operating system. Code was written in RATFOR and adapted some routines available in FORTRAN (Press et al., 1986). The random number generator was the standard DEC PDP-11 FORTRAN 77/RT-11 RAN function passed through a shuffling routine to remove sequential correlations (Binder & Heermann, 1988). Graphic output and some portions of the data analysis were performed with PLOT software from New Unit, Inc., Ithaca, NY.

Theory

Fluorescence Quenching in a Membrane. A theory for the quenching of fluorophores in a membrane may be developed from theories of isotropic solution quenching. Several details specific to the anisotropic structure of the membrane are incorporated into the theory, including the observation that the membrane bilayer in the fluid, liquid-crystalline phase is a partially ordered two-dimensional hexagonal lattice of acyl chains (Janiak et al., 1976, 1979; Luzzati, 1968; Ruocco & Shipley, 1982), and that the lateral diffusion coefficients of phospholipids and membrane-bound fluorophores in a bilayer are much smaller than diffusion coefficients in isotropic low-viscosity solutions (Jovin & Vaz, 1989). The fluorescence lifetimes are assumed to be short relative to the mean residence time of an acyl group in a lattice site (Galla et al., 1979; Haugland, 1989). Finally, the interaction of fluorophore with quencher is sufficiently short range to require contact, so that only the quenchers located at positions of the membrane lattice surrounding the fluorophore can contribute to quenching (London & Feigenson, 1981a).

The rate processes for the decay of a fluorophore in the excited state are described by rate constants for fluorescence (k_f), nonradiative (k_n), and quenched (k_q) decay. We assume that the second-order rate constant k_q simply adds to the total decay rate, and that the presence of the quencher has no effect on the first-order rate constants k_f and k_n. We also assume that any orientation effects on quenching are averaged over the lifetime of the fluorophore such that all sites around the fluorophore are essentially equivalent. This is a reasonable supposition for small organic molecules and phospholipid acyl chains with rotational correlation times less than the fluorescence lifetime (Mulders et al., 1986; Straume & Litman, 1987; Stubbs et al., 1981).

Under these conditions we consider each quenching chain to contribute additively to the total quenching rate: for a single fluorescent molecule, the total rate equals Jk_q, where J is the number of quenching acyl chains interacting with the fluorophore during its excited-state lifetime (i.e., occupying neighboring, interacting sites), and k_q is the intrinsic quenching rate for a single quencher. Thus, the steady-state fluorescence, F_J, for a given occupancy of quenchers, J, is given by

$$F_J = I_0 k_f/(k_f + k_n + Jk_q) \quad (1)$$

where I_0 is a constant including all instrumental factors. The "single-chain" fluorophores used in this study are considered to occupy one site on a two-dimensional average hexagonal lattice of *acyl* chains in the liquid-crystalline state. There are then two cases to consider in this model: (1) the quenching phospholipid contains a quenching moiety on one acyl chain (BrPC and SpinPC) or (2) both acyl chains on the phospholipid are quenchers (di-BrPC and di-SpinPC).

In addition, there is an important consideration concerning the *dependence* of sites around the fluorophore: the quenchers

used here are diacyl phospholipids, not fatty acids, and therefore each phospholipid molecule occupies *two* sites on an acyl lattice, which, in effect, correlates the occupancy of one site by the quenching chain and a neighboring site by the sister chain. We term this treatment the *dependent-site model*. When neighboring site dependence is ignored, we term the treatment the *independent-site model*.

We start with a general derivation, applicable to both the independent- and dependent-site models. A fluorescence-quenching experiment yields two limiting fluorescence values that establish a relation between fluorescence intensity and k_q. In a membrane with no quencher the measured fluorescence, F, equals F_0 since $J = 0$. A membrane composed entirely of quenching lipid will yield a value for F_M, where $J = M$, and M is the maximum number of nearest neighbors that may be occupied by a quencher for a given lattice. From eq 1 and the definitions of F_0 and F_M

$$F_M/F_0 = (k_f + k_n)/(k_f + k_n + Mk_q) \quad (2)$$

$$k_q = (k_f + k_n)(F_0 - F_M)/MF_M \quad (3)$$

The fluorescence lifetime in the absence of quencher is defined as $\tau_0 = 1/(k_f + k_n)$, thus from eq 3

$$k_q = (F_0 - F_M)/\tau_0 MF_M \quad (4)$$

The fluorescence of each occupied state, F_J (for $J = 0$–M), in terms of F_0 and F_M, is given by eq 1, eq 3, and the definitions of F_0 and F_M:

$$F_J = \frac{F_0}{1 + \frac{J}{M}\frac{(F_0 - F_M)}{F_M}} \quad (5)$$

Each *phospholipid* site B around a fluorophore is considered independent and participates in an exchange equilibrium between unlabeled lipid L and quenching lipid Q:

$$Q + BL \rightleftharpoons L + BQ; \quad K_a = \frac{[L]\,[BQ]}{[Q]\,[BL]} \quad (6)$$

where K_a is the apparent relative binding constant of a quenching phospholipid for the site[3] (East & Lee, 1982; London & Feigenson, 1981a). From eq 6 and mass balance relations for the membrane components, the concentration of sites occupied by a quenching phospholipid in terms of the mole fraction of quenching phospholipid (χ) in the total composition is

$$[BQ] = \frac{K_a(\chi)}{1 + (\chi)(K_a - 1)} \quad (7)$$

The total probability for a site to be occupied by either type of lipid is [BQ] + [BL] = 1. Each site has a probability [BQ] for occupancy by a quenching lipid, with [BQ] equal to χ if there is no preferential binding. Consequently, each site has a probability 1 − [BQ] = [BL] to be free of quencher. The model membranes in this study are composed only of PC and so we do not expect probe fluorophore preference for quenching or nonquenching PC as a result of head-group interactions (Caffrey & Feigenson, 1981; London, 1980; London & Feigenson, 1981b). Preferential interactions based on lipid acyl chain characteristics are possible, but are not considered here.

Independent-Site Model. A statistical description of quencher distributions, or "occupancy states", around each fluorophore in a large ensemble of fluorophores may be calculated for all mole fractions of quencher. For a given occupancy state having J and only J sites occupied out of a possible maximum of M, regardless of arrangement, the probability for each state P_J is a combination of M items taken J at a time multiplied by the probability for occupancy of a single site by a quencher, which is given by a binomial distribution

$$P_J = \frac{M!}{J!(M - J)!}[BQ]^J(1 - [BQ])^{M-J} \quad (8)$$

A general equation for relating the observed fluorescence at a given mole fraction (χ) of quenching lipid, F_χ, to the quencher occupancy distribution function, P_J, and the fluorescence associated with that state, F_J, for M total sites is

$$F_\chi = \sum_{J=0}^{M} P_J F_J \quad (9)$$

Combining eqs 5, 7, and 8, the total fluorescence as a function of χ for the independent-site model is

$$F_\chi = \sum_{J=0}^{M} \frac{M!}{J!(M - J)!}[BQ]^J(1 - [BQ])^{M-J}\left(\frac{F_0}{1 + \frac{J}{M}\frac{(F_0 - F_M)}{F_M}}\right) \quad (10)$$

F_M is a measure of the efficiency of quenching and is obtained directly from a fluorescent quenching experiment only when both chains of the quenching phospholipid contain quenching groups and the membrane is composed completely of quenching lipid ($\chi = 1$) so that *all* M sites on the lattice around the fluorophore are occupied by quencher. A larger F_M corresponds to a lower efficiency of quenching (i.e., smaller k_q).

Single-Chain Quenchers. In the case of a diacyl phospholipid with only one quenching chain, F_M must be calculated from the observed fluorescence at $\chi = 1$, F_M^{obs}, since the concentration of quenching chains is half the total. F_M is calculated numerically by the iterative method of bisection (Press et al., 1986) from

$$F_M^{obs} - \sum_{J=0}^{M} \frac{P_J F_0}{1 + \frac{J}{M}\frac{(F_0 - F_M)}{F_M}} = 0 \quad (11)$$

where P_J is the occupancy distribution of quenching chains when $\chi = 1$. Equation 11 is used for the calculation of F_M in both the independent-site and dependent-site models.

Dependent-Site Model. The assumption of quenching-site dependence or independence has an effect only on the probability distribution P_J in the relations derived above. For the independent case, P_J is a binomial distribution (eq 8). If entire phospholipids are considered as the independent quenching units, then F_M always equals F_M^{obs} for both single- and double-chain quenchers. The phospholipid "lattice", however, actually consists of randomly oriented but covalently linked acyl pairs on a hexagonal *acyl* lattice. A more realistic description of the molecular details of quenching must include this structural constraint since the quenching groups on the

[3] Lipid mole fractions are used, and any activity coefficients differing from unity are contained in the value of K_a. The concepts of binding site and relative affinity are perhaps more meaningful when used to describe specific interactions of a small ligand with a larger molecule; here we use the term "binding site" to mean a site that is nearby and referenced to another site occupied with a probe, in this case a fluorophore of about the same dimensions as the neighboring phospholipids.

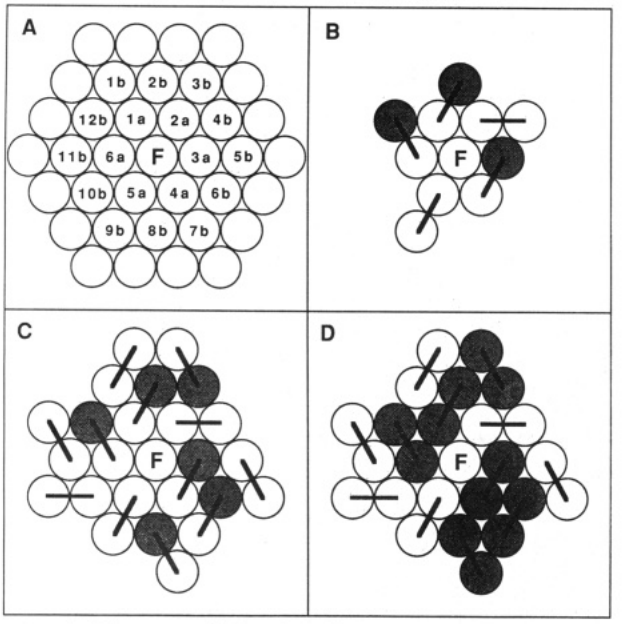

FIGURE 1: Placement of phospholipids by a Monte Carlo algorithm on a hexagonal acyl chain lattice. (A) Scheme used to index the placement of phospholipids and their acyl chains. Letters a and b correspond to the first and second shell of neighbors of the fluorophore (center site labeled F). Only two neighbor shells are labeled here. (B) Representative first-neighbor shell filled by the Monte Carlo algorithm. The membrane is composed of 0.5 mole fraction of a single quenching chain phospholipid. Each phospholipid is represented by two acyl sites connected with a thick black line. Quenching chains are shaded dark; unlabeled chains are light. (C) Same as B with second shell filled. (D) same as C except double-chain quenching phospholipid substituted for the single-chain quencher.

phospholipids each occupy an acyl site.

"Dependence" refers to the mutual effect of each sister acyl chain of a phospholipid on the occupancy of a neighboring lattice site. The sister chain *must* occupy a neighboring position, and this necessity reduces the possible arrangements of other phospholipids neighboring that site. A quantitative description accounting for the effect of phospholipid chain site dependence on nearest-neighbor distributions around a probe lattice site cannot be posed in a readily soluble analytic form: the situation is analogous to the dimer adsorption problem examined theoretically for a square lattice (Fisher, 1961). Monte Carlo techniques, however, are ideal for enumerating by brute force the states of complex systems when an analytic expression is not available (Binder & Heermann, 1988) and are used here to solve for the concentration-dependent distributions of single- and double-chain phospholipid quenchers around a fluorophore.

A Monte Carlo algorithm was used to place phospholipids on a hexagonal acyl lattice surrounding a fluorophore occupying a single lattice site (Figure 1). The first shell of nearest neighbors was filled initially (sites 1a–6a) followed by the second shell (sites 1b–12b) by the following protocol: for a given mole fraction of quenching phospholipid a random number is generated, with uniform deviance, between 0 and 1. If the number is less than the mole fraction of quenching lipid, then the first site (1a) is tagged as being occupied by one of the chains of a quenching lipid. In the case of a single-chain quencher, a second number is generated, and if it is less than $^1/_2$, then the site 1a is considered to be occupied by the quenching chain. With the double-chain quencher this site must be occupied by a quenching chain. The sister chain of the phospholipid is then placed by counting the remaining unoccupied lattice sites (five in this case; i.e., sites 6a, 12b, 1b, 2b, and 2a), generating a random number between 0 and 1 and assigning the chain to one of the sites depending on which Nth random interval is generated, where N is the number of possibilities available. The algorithm then proceeds to the next site, 2a (which had a $^1/_5$ chance of already being occupied by one of the chains of the phospholipid associated with site 1a) and, if unoccupied, again goes through the sequence of random number generation to place both the chains. After the first shell of nearest neighbors is filled (Figure 1B), the remaining unoccupied sites of the second shell are filled (Figure 1C). Further shells can be filled with the same algorithm,[4] but only two filled shells are considered in this work (or a partially filled shell with $M = 12$—see Discussion). After filling is complete, the indexed sites are counted according to their occupancy by a quencher, the total ranging from 0 to the maximum number of sites.[5] A bin corresponding to the total is incremented, the number of bins equal to $M + 1$ (i.e., 0–M). The sequence is repeated 50000 times, and the statistics for the probability of occupancy are calculated for each bin as the (bin total)/(total iterations).

Lifetime Distribution Model. The quenching model may be converted to a fluorescence lifetime distribution model if fluorescence lifetimes are substituted for fluorescence intensities. The assumption that $F/F_0 = \tau/\tau_0$ for each fluorescent molecule arises from the original postulate that the rate of deactivation is dependent on the number of quenchers. Substituting into eq 5

$$\tau_J = \frac{\tau_0}{1 + \frac{J}{M}\frac{(\tau_0 - \tau_M)}{\tau_M}} = \tau_0(F_J/F_0) \qquad (12)$$

which is readily calculated if τ_0 is known, and gives the lifetime associated with each occupied state. Each (τ_J, P_J) pair is a point on a fluorescence lifetime distribution curve.

RESULTS

Phosphatidylcholine Synthesis. The brominated PC products were pure by TLC and ran with the same mobility as the parent lipids in basic and neutral systems. ^{1}H NMR spectroscopy was used to quantitate the extent of bromination (Reinert et al., 1978) and the presence of side products. All resonance frequencies and integrated peak intensities were as expected: complete loss of the oleate vinyl resonance at δ = 5.3 (4 per DOPC, 2 per POPC), complete loss of the allylic proton resonances at δ = 2.0 (8 per DOPC, 4 per POPC) and their reappearance as resonances neighboring a halogenated carbon at δ = 1.8 ($C\underline{H}_2CHBrCHBrC\underline{H}_2$; ~8 per DOPC, ~4 per POPC), and resonances on the halogenated carbon at δ = 4.2 ($C\underline{H}BrC\underline{H}Br$). No other spectral changes were seen compared to the parent PC spectrum, indicating that the bromination was specific for the oleate double bond.

Di-SpinPC was >95% pure as judged by TLC. The major spot had a mobility slightly greater than that of POPC or SpinPC in the neutral system, and had a small "cap" of phosphate-positive lipid that is suspected to be the 1,3-diacyl isomer of the phospholipid (Lammers et al., 1978). EPR

[4] The total number of sites and the computation time increase as $\sum_{L=1}^{K} 6L$, where K is the number of neighbor shells considered.

[5] In some cases this is not always true, as with $K = 2$; single-chain quenchers can have a maximum of 6 in the first shell, but the second shell will sometimes be less than the maximum (12) because of the non-quenching sister chain occupancy from the first shell, and thus the total will always be less than the maximum number of sites (18). This is not a problem, however, since the Monte Carlo algorithm properly counts these cases.

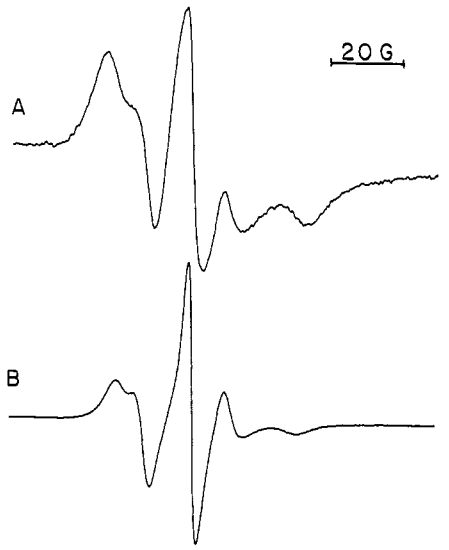

FIGURE 2: EPR spectra of the spin-labeled phospholipids used as fluorescence quenchers. (A) Di-SpinPC in POPC, probe to lipid ratio, 1:1000. (B) SpinPC in POPC, probe to lipid ratio, 1:500.

spectra of multilayers of dilute di-SpinPC incorporated into POPC revealed a typical bilayer appearance (Marsh, 1981) together with several features that differ in comparison to the spectrum of singly labeled SpinPC (Figure 2). There is evidence of line broadening, probably due to Heisenberg spin-exchange together with dipolar interactions between the labeled chains (Eastman, et al., 1969). The outer hyperfine splitting is 54 G, an increase from 49 G for SpinPC, implying motional restriction and/or reduced rates of motion (Freed, 1976). There was no sharp, three-line spectral component that would have indicated aqueous solubility of the di-SpinPC or the presence of labeled fatty acid, even in dispersions of pure di-SpinPC (data not shown).

DPH-PC was pure by TLC and had the same mobility as a PC standard. Fluorescence excitation and emission spectra were as previously described (Parente & Lentz, 1986).

Predictions of the Theory. (A) Independent Lattice Sites. Theoretical quenching curves for the independent-site model (eq 10) are illustrated in the plots of Figure 3. This model describes either entire phospholipids each occupying a single, independent site, or free acyl chains occupying single, independent lattice sites. Figure 3A shows how different efficiencies affect the theoretical plots of fluorescence vs mole fraction of quenching lipid. Noticeable differences are seen in the amounts of "residual", or unquenched, fluorescence in the membrane when composed *entirely* of quenching lipid. The quenching curves become progressively more shallow as the quenching efficiency decreases (F_M increases). The limiting case when $F_M = 0$ (bottom curve, Figure 3A) is equivalent to the analysis of London and Feigenson (1981a): the fluorescence is completely quenched by contact with one quencher, i.e., an approximation of eq 10: $P_0 = (1 - \chi)^M$, and the calculated fluorescence is then $F_\chi = F_0 P_0$. The effect of M, the maximum number of quenching neighbors, on the calculated quenching curves is shown in Figure 3B. A prominent trend is that the sensitivity of the quenching to M (i.e., the absolute difference between the curves) decreases as the quenching becomes less efficient.

(B) Dependent Acyl Lattice Sites. Monte Carlo simulations are needed to solve for the distributions of quenchers in the case of nonindependence of the placement of phospholipid acyl chains on the acyl lattice. The adequacy of random number generation was demonstrated by modifying our Monte Carlo algorithm to generate a distribution for *independent* lattice

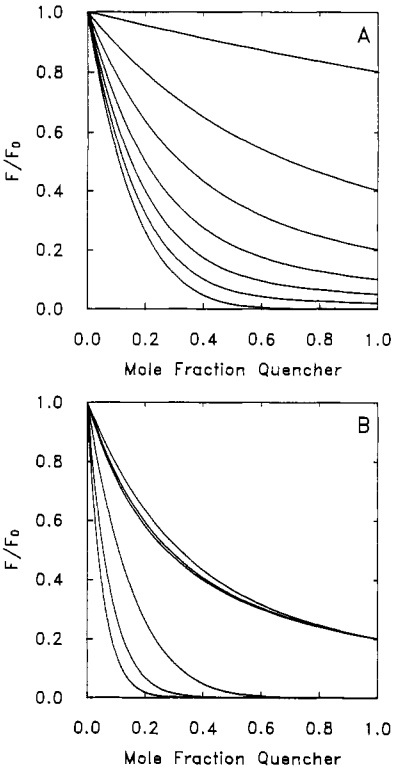

FIGURE 3: Calculated quenching curves for the *independent-site model* as a function of the mole fraction of quenching species. The ordinate is relative fluorescence, F/F_0, and the abscissa is the mole fraction of quenching species. Curves are calculated by use of eq 10. (A) Effect of inefficient quenching (residual fluorescence), F_M. Each curve in the family has a fixed number of nearest neighbors, $M = 6$, and no preference for the binding of quenching vs nonquenching species (relative affinity constant, $K_a = 1$). Fluorescence in pure quencher has the value F_M, and curves are plotted for $F_M = 0.0$, 0.02, 0.05, 0.1, 0.2, 0.4, and 0.8. (B) Effect of number of nearest neighbors $M = 6$, 12, and 18 at $F_M = 0.2$ (upper three curves) and $F_M = 0.0$ (lower three curves). Steeper curves in each family correspond to larger M.

sites and comparing the results to a binomial distribution calculated with eq 8. Results for 50 000 iterations showed that, for $M = 6$, the Monte Carlo enumerations for each occupancy state converged to within 1% of the calculated binomial probability (data not shown). This accuracy is sufficient so that fluorescence quenching curves generated from both distributions are visibly identical. For the fitting of quenching curves to the data presented in this paper, we generated distributions for $M = 6$, 12, and 18, stepping 0.02 mole fraction unit from 0 to 1. For $M = 12$, the distribution was counted as for $M = 18$ (two shells of nearest neighbors) except that the odd-numbered positions in the second shell (1b, 3b, ...) were ignored in the enumeration (see Figure 1).

Figure 4 illustrates theoretical quenching curves for the dependent-site model for both a single-chain quencher and a double-chain quencher. For comparison, the *independent*-site model is also plotted (dotted line) with identical spectral parameters. As with the independent-site model (Figure 3), the same patterns are seen with respect to M and to quenching efficiency. Dependent-site simulations for both single- and double-chain quenchers always show less steep quenching when compared with the independent-site model. Note that it is easier to distinguish differences between the models when M is small.

Observed Quenching of Fluorescent Probes. The quenching theory was tested by examining several fluorescent probes in membranes where two critical parameters of the theory could be manipulated experimentally: (1) the efficiency of quenching, which depends on both the chemical nature of the

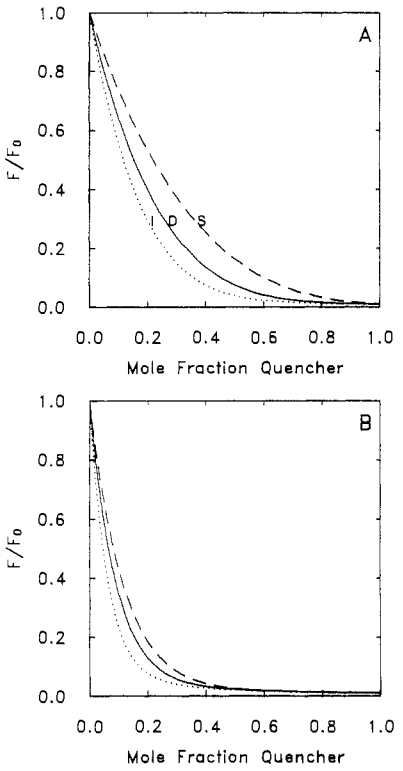

FIGURE 4: Theoretical quenching curves for the *dependent-site model* calculated from distributions generated by a Monte Carlo algorithm. (A) All curves are calculated from the spectral parameters $F_0 = 1.0$, $F_M = 0.1$, and with $M = 6$. Dashed line is the quenching curve for a single-chain quencher (labeled S), solid line is the double-chain quencher (labeled D). For reference, the dotted line is generated from the independent model by use of eq 10 (labeled I). (B) Same as A except that the distribution for $M = 18$ was used. The slight bumpiness of the curves results from the fluctuations inherent in finite Monte Carlo simulations.

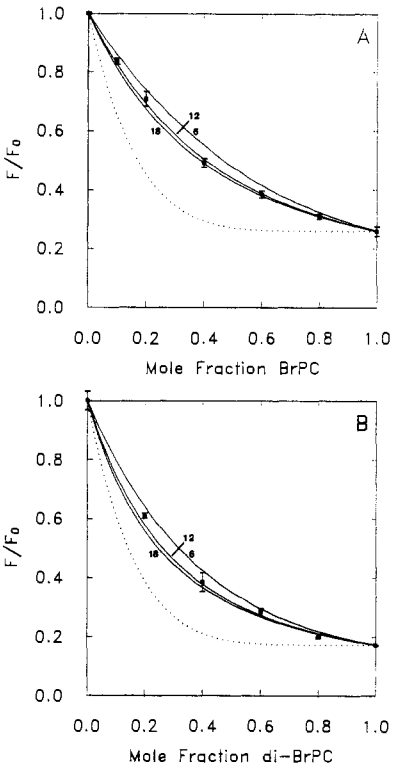

FIGURE 5: Quenching of tryptophan octyl ester (TOE) by brominated phospholipids in POPC. Fluorescence is expressed as F/F_0. (A) Quenching by BrPC (single-chain quencher), $F_M^{obs} = 0.26$. The solid curves are calculated from the dependent-site model for single-chain quenchers, $M = 6$, 12, and 18. The dotted line is calculated with eq 13 (London & Feigenson, 1981a) using $M = 6$ (see text). (B) Quenching by di-BrPC (double-chain quencher), $F_M^{obs} = 0.17$. Fitting parameters as in A except that distributions are generated for double-chain quenchers.

quencher (either a bromine or a nitroxide moiety) and the type of fluorophore used; and (2) the neighbor quencher distribution around the probe, which depends on the use of a double- or single-chain quenching phospholipid and the constraints imposed by an assumed lattice structure.

Brominated and spin-labeled compounds both quench tryptophan fluorescence, but with markedly different efficiencies. TOE was incorporated into PC multilayers containing brominated PC and the results are shown in Figure 5A (BrPC) and 5B (di-BrPC). Quenching curves calculated for the dependent-site model are drawn from $M = 6$, 12, and 18. With the independent-site model (eq 10), the best fit corresponds to $M = 6$ for both brominated lipids and closely matches the dependent site model curve for $M = 12$ (data not shown). Analysis of the quenching curves using eq 13 (London & Feigenson, 1981a)

$$(F - F_{min})/(F_0 - F_{min}) = (1 - \chi)^M \qquad (13)$$

illustrates the inadequacy of neglecting the "residual" fluorescence (F_{min}). For $M = 6$, eq 13 yields a theoretical line that deviates significantly from the data (see Figure 5A,B). The number of nearest-neighbor phospholipids has been reported to be 6 for similarly sized fluorophores (London & Feigenson, 1981a) whereas use of eq 13 results in a poor fit to $M = 2$ or 3 (not shown).

Figure 6 shows the fluorescence of TOE in mixtures with the spin-labeled quenchers. Figure 6A shows quenching by SpinPC, the single-chain quencher, and Figure 6B shows the results for the double-chain quencher, di-SpinPC. For both quenchers, the dependent-site model generates curves with very similar shape and qualitative appearance for exactly the same number of nearest neighbors, even though the double quencher has significantly steeper concentration dependence than does the single-chain quencher. The insets of Figure 6A and B, however, illustrate that the independent-site model predicts a significantly *different* number of phospholipid nearest neighbors for the two different types of quenching lipid: for the single-chain quencher, $M = 6$; for the double-chain quencher, $M = 9$. For both the single and double quenchers there is a consistent shift from $M = 18$ to $M = 12$ for the dependent-site model as the mole fraction of quenching lipid increases (the curve for $M = 6$ deviates significantly from the data and is not shown). For the brominated quenchers (Figure 5) the difference between the $M = 12$ and $M = 18$ curves is too small to make a distinction with the given data, but $M = 6$ does not fit the data.

TMA-DPH is quenched appreciably by the nitroxide spin-labeled phospholipids, but not by brominated lipids. Figure 7 shows the results for TMA-DPH in mixtures with SpinPC and di-SpinPC. The quenching profiles of the dependent-site model are quite similar to those for TOE: all the data lie between $M = 12$ and $M = 18$, with a smooth monotonic shift from $M = 18$ to $M = 12$ as the concentration of quencher increases. The independent-site model gives a best fit of $M = 7$ for SpinPC and $M = 10$ for di-SpinPC, again quite similar to the TOE results.

Figure 8 presents the results for DPH-PC quenching. This fluorophore differs from the others used in this study because the fluorescent DPH-propionic acid is esterified to a phospholipid and thus always neighbors an unlabeled sister chain. Again, the data lie between the calculated lines for $M = 12$

Table I: Discrete Lifetime Distributions from Fluorescence Quenching Theory, Fit with Continuous Distributions[a]

		discrete[b]		Gaussian[c]		Lorentzian[c]	
F_M	χ	center	width[d]	center	width[d]	center	width[d]
0.8	0.02	9.9	0.5	10.3	0.9	9.9	0.2
	0.10	9.7	0.7	9.8	0.9	9.9	0.6
	0.20	9.5	0.7	9.6	0.8	9.6	0.6
	0.40	9.3	0.7	9.3	0.7	9.3	0.6
	0.50	9.2	0.7	9.2	0.7	9.2	0.5
	0.60	9.1	0.6	9.1	0.6	9.1	0.5
	0.80	8.8	0.5	8.8	0.5	8.8	0.4
0.5	0.02	9.7	1.6	10.0	2.2	9.6	0.7
	0.04	9.4	2.1	10.1	2.9	9.4	0.6
	0.10	9.0	2.3	9.4	2.7	9.4	1.6
	0.16	8.7	2.1	9.0	2.3	9.0	2.0
	0.30	8.0	2.1	8.1	2.2	8.1	1.7
	0.40	7.6	1.9	7.7	1.9	7.7	1.6
	0.60	7.1	1.5	7.2	1.5	7.1	1.2
	0.80	6.5	1.2	6.5	1.2	6.5	0.9
0.1	0.02	8.9	5.7	7.5	3.9	9.6	3.6
	0.04	8.0	7.3	7.3	4.4	8.0	2.0
	0.20	4.5	5.8	4.2	2.7	4.2	1.4
	0.30	3.5	4.2	3.8	2.8	3.8	2.6
	0.40	2.9	3.0	2.9	1.9	3.0	1.7
	0.50	2.5	2.2	2.5	1.4	2.5	1.3
	0.60	2.3	1.6	2.3	1.2	2.3	1.0
	0.80	1.7	0.8	1.7	0.7	1.7	0.6

[a] Parent fluorescence probability distribution given by $M = 18$, dependent model, single acyl chain quencher, $\tau_0 = 10$ ns. Residual fluorescence, F_M, and mole fraction quencher, χ, transformed to a lifetime distribution by use of eq 12. Lifetimes are in ns. [b] Center (μ) and standard deviation (σ) of the discrete distribution calculated from $\mu = \sum_{J=0}^{M} \tau_J P_J$, $\sigma^2 = \sum_{J=0}^{M} [(\tau_J - \mu)^2 P_J]$ where τ_J is the lifetime associated with the population density P_J. [c] μ, σ, and the maximum P_J from the discrete distribution statistics are used as starting estimates for a nonlinear least-squares fit of the center, width, and amplitude to Gaussian and Lorentzian continuous distributions (see eqs 14 and 15 in the text). The weighting of the data for chi-square minimization was constant for all points. [d] Full-width at half-maximum (2.354σ for the Gaussian). The width of the discrete distribution is also given as 2.354σ.

and $M = 18$, as with TMA-DPH and TOE. The best M values for the independent-site model are $M = 7$ for SpinPC and $M = 10$ for di-SpinPC. Apparently, this quenching method cannot discern the effect of the single unlabeled sister chain on the quenching characteristics of the probe if we compare its behavior to TMA-DPH.

Lifetime Distribution Model. A model of spatial distributions of quenchers on a lattice surrounding a fluorophore can be converted directly into a model of fluorophore lifetime distributions by means of eq 12. In this model, each occupancy state of the ensemble of fluorophores gives rise to a single-exponential lifetime with an amplitude given by its population density. To illustrate, consider a fluorophore that has a single-exponential lifetime of 10 ns in a pure phospholipid "A", and a lifetime of 5 ns (equivalent to an $F_M = 0.5$ relative to lipid A) in phospholipid "B". Phospholipid B may be either a quencher or a normal phospholipid in which the fluorophore has a lower quantum yield relative to A. The probability distribution, P_J, at a given mole fraction may be obtained either from the independent-site model (eq 8) or from the Monte Carlo simulations for the dependent-site model. Figure 9 shows the calculated lifetime distribution in a binary system of these lipids in which for lipid B, $\chi = 0.5$ (Figure 9A), and $\chi = 0.2$ (Figure 9B). These discrete distributions were fitted with both Gaussian and Lorentzian theoretical distributions (i.e., they were not recovered from actual fluorescence decay rates) in order to show the similarity of our calculated discrete distributions to continuous distribution models (Alcala et al., 1987; Gryczysnki et al., 1988; Lakowicz et al., 1987a; Williams & Stubbs, 1988). The Gaussian function, $G(\tau)$, is given by

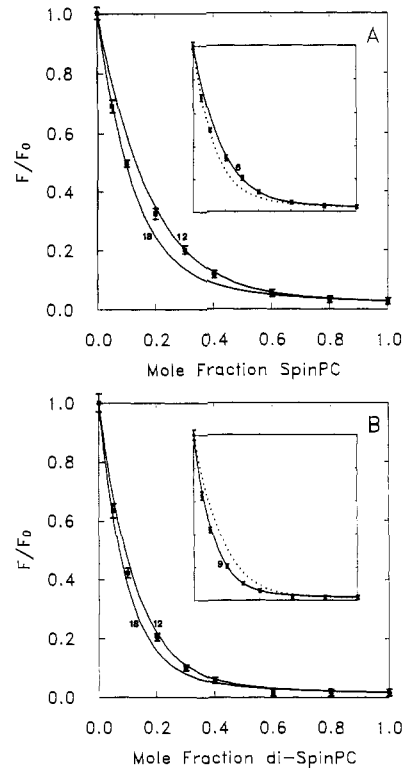

FIGURE 6: Quenching of tryptophan octyl ester (TOE) by spin-labeled phospholipids in POPC. (A) Quenching by SpinPC (single-chain quencher), dependent-site model. Top curve, $M = 12$; bottom curve, $M = 18$; $F_M^{obs} = 0.025$. Inset shows best fit for the independent-site model, giving $M = 6$ (solid line); dotted line shows $M = 9$ for comparison (see Discussion). (B) Quenching by di-SpinPC (double-chain quencher). Same values of M as in A except $F_M^{obs} = 0.016$. Inset shows best fit for the independent-site model, giving $M = 9$ (solid line); dotted line shows $M = 6$ for comparison (see Discussion).

$$G(\tau) = \frac{A}{\sigma\sqrt{2\pi}} \exp\left[-\frac{1}{2}\left(\frac{\tau - C}{\sigma}\right)^2\right] \quad (14)$$

and the Lorentzian function, $L(\tau)$, is

$$L(\tau) = \frac{A}{\pi} \frac{W/2}{(\tau - C)^2 + (W/2)^2} \quad (15)$$

where A is the amplitude, W is the full-width at half-maximum, C is the center, and σ is the standard deviation of the Gaussian. Table I summarizes the results for a number of discrete distributions calculated for binary mixtures with a range of mole fractions and relative fluorescence quantum yields. With the arbitrary assumption of constant weighting for all data points, the Gaussian distribution always gives a better fit than the Lorentzian distribution (i.e., the reduced chi-square for the Lorentzian was always several times higher than that for the Gaussian).

Discussion

In this paper, we develop a theoretical treatment for the quenching behavior of small amphipathic fluorescent probes in a membrane consisting of mixtures of quenching and non-quenching phospholipids. This treatment improves on existing theories by (1) accounting in a physically reasonable way for inefficient quenching and (2) depicting an essential feature of the structure of the membrane to be a lattice of acyl chains. The quenching analysis of London and Feigenson has provided a simple and intuitive description of fluorescence quenching in a membrane: a quenching process dominated by the contact,

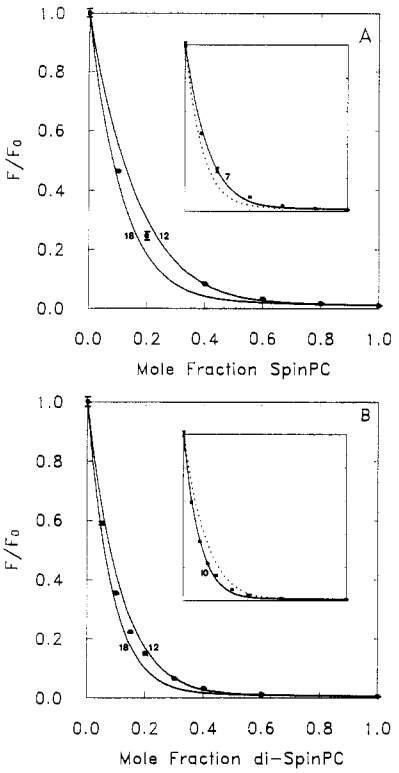

FIGURE 7: Quenching of TMA-DPH by spin-labeled phospholipids in POPC. (A) Quenching by SpinPC, dependent-site model. Top curve, $M = 12$; bottom curve, $M = 18$; $F_M^{obs} = 0.0096$. Inset is best fit for the independent-site model, giving $M = 7$ (solid line); dotted line shows $M = 10$ for comparison. (B) Quenching by di-SpinPC. Same values of M as in A except $F_M^{obs} = 0.0043$. Inset shows best fit for the independent-site model, giving $M = 10$ (solid line); dotted line shows $M = 7$ for comparison.

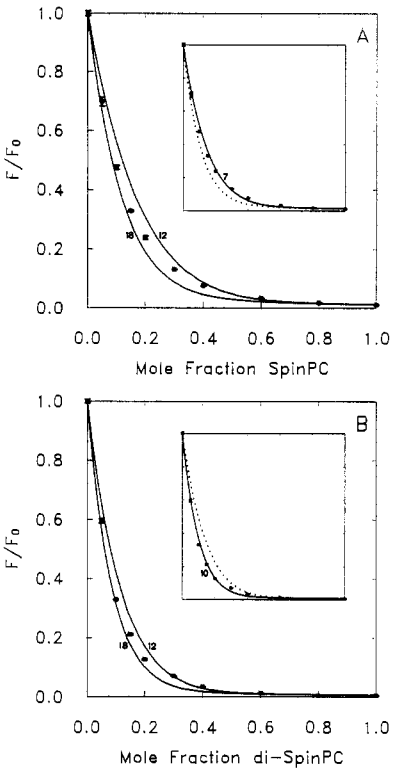

FIGURE 8: Quenching of DPH-PC by spin-labeled phospholipids in POPC. (A) Quenching by SpinPC, dependent-site model. Top curve, $M = 12$; bottom curve, $M = 18$; $F_M^{obs} = 0.011$. Inset is best fit for the independent-site model, giving $M = 7$ (solid line); dotted line shows $M = 10$ for comparison. (B) Quenching by di-SpinPC. Same values of M as in A except $F_M^{obs} = 0.0046$. Inset shows best fit for the independent-site model, giving $M = 10$ (solid line); dotted line shows $M = 7$ for comparison.

or near contact, of the quenching species with the fluorophore. This theory is sufficient when *relative* quenching is used, as for the determination of lipid–protein binding constants and fluorophore depth (Blatt & Sawyer, 1985; Chattopadhyay & London, 1987; London & Feigenson, 1981b). Also, partition of a fluorophore between coexisting fluid and gel phases can be properly determined, since only the intensity of fluorescence at the phase boundaries is important. However, this theory is weakest in describing the residual fluorescence in a bilayer of pure quenching lipid as arising from inaccessible fluorophores. This simplification may indeed be true for the quenching of membrane-bound proteins containing more than one fluorophore, but the analysis fails for small, *exposed* fluorophores whenever there is a large residual fluorescence in a membrane composed entirely of quenching lipid. We show in this paper that the assumption that contact of the quencher with the fluorophore results in a dark complex, i.e., instantaneous deactivation of the excited state, is not a necessary assumption. Instead, residual fluorescence, or inefficient quenching, can be accounted for by a real physical process of competing rates of deactivation. The analysis of London and Feigenson (1981a) cannot fit this residual fluorescence with a reasonable number of nearest neighbors for a fluorophore occupying a single acyl lattice site (dotted lines, Figure 5).

The quenching of fluorophores in a membrane may be considered as a special case of solution quenching. Unlike quenching in an isotropic, low-viscosity solution, however, there are, within the partially ordered two-dimensional lattice of a liquid-crystalline membrane, constrained steric relationships and orientations that limit the number of possible interactions. We have chosen to examine amphipathic probes so that there exists a defined orientation relative to the phospholipids. TOE is oriented with Trp located at the aqueous interface (Jain et al., 1985). TMA-DPH is also oriented with the trimethylamino group at the head-group region (Prendergast et al., 1981), and DPH-PC behaves like a phospholipid (Parente & Lentz, 1986). DPH, another popular fluorescent probe, has no polar groups and appears to be located in different regions of the bilayer (Mulders et al., 1986; Straume & Litman, 1987) and is therefore more difficult to treat because of the additional environmental heterogeneity.

Our analysis benefits from simplifications based on current knowledge of membrane order: (1) the membrane is an anisotropic, two-dimensional ordered lattice of acyl chains with a predictable nearest-neighbor acyl lattice structure (Janiak et al., 1976; Luzzati, 1968; Ruocco & Shipley, 1982); and (2) given a typical lateral diffusion coefficient for phospholipids in membranes of $D = 2 \times 10^{-8}$ cm^2 s^{-1} (Devaux & McConnell, 1972; Jovin & Vaz, 1989), the mean time between jumps of a phospholipid molecule from one lattice point to the next, with a lattice spacing $\lambda = 0.8$ nm, is $t = \lambda^2/4D = 80$ ns (Galla et al., 1979). With fluorescence lifetimes of 10 ns or less, it is a good approximation to assume no exchange of sites during the lifetime of the fluorophore. Furthermore, the fluorophore–quencher interaction distance has been found to be in the range 5–7 Å in solvents and 10–11 Å in membranes (Green et al., 1973; London & Feigenson, 1981a; Medinger & Wilkinson, 1965). Thus, it is reasonable to expect that only the *nearest-neighbor* heavy-atom and free-radical quenchers in contact with the fluorophore can quench fluorescence.

Other theoretical treatments of quenching in two dimensions concern resonance energy transfer, which occurs over much greater distances than does contact quenching (Dewey & Hammes, 1980; Estep & Thompson, 1979; Fung & Stryer,

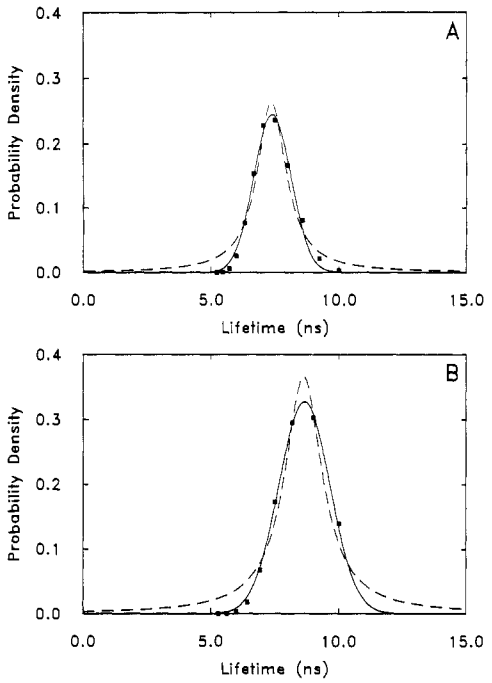

FIGURE 9: Theoretical lifetime distributions generated from theoretical quencher probability distributions. (A) The fluorescence lifetimes are calculated with eq 12 ($F_M = 0.5$, $\tau_0 = 10$ ns). The corresponding probability distribution was obtained from a Monte Carlo simulation for the dependent-site model: $\chi = 0.5$, $M = 18$, single-chain quenching phospholipid. The solid curve is a best fit to a Gaussian distribution (center, 7.40 ns, FWHM, 1.71 ns), the dashed curve is a best fit to a Lorentzian distribution (center, 7.38 ns, FWHM, 1.37 ns). The reduced chi-square for the Lorentzian is 5.5 times higher than the Gaussian with constant weighting of all the data (see Table I). Even though there are 19 occupancy states for $M = 18$, only 12 points are plotted since 7 states do not occur for single-chain quenchers with site dependence. (B) Same as A except $\chi = 0.2$, and the corresponding probability distribution was used. Gaussian fit: center, 8.66 ns, FWHM, 2.35 ns. Lorentzian fit: center, 8.63 ns, FWHM, 1.79 ns.

1978; Snyder & Freire, 1982; Wolber & Hudson, 1979). For some solutions of the problem, there is a requirement for *uniform* distributions of quenchers (acceptors), i.e., the number of quenchers in the area surrounding a fluorophore is constrained to equal the area times the bulk concentration (Dewey & Hammes, 1980; Fung & Stryer, 1978; Wolber & Hudson, 1979). In the theory of Estep and Thompson (1979) there is no restriction on the number of quenchers around a fluorophore, but an approximation is used that all the quenchers are at the same distance from the fluorophore. Snyder and Freire (1982) avoided these approximations by using Monte Carlo simulations to calculate quenching curves and found that the analytic solution of Wolber and Hudson (1979) gave identical results if excluded-volume effects were not included in the simulations. These results suggest that, for most resonance energy transfer situations, it is not necessary to consider a lattice of discrete sites available to the fluorophore and the quencher. It is sufficient to consider the fluorophore–quencher separation as a continuum, described by an average quencher concentration. Our analysis differs from these others in that we address the problem of short-range contact quenching with high concentrations of quencher and so must account for local order and site dependence (i.e., excluded-volume effects). Unlike the analytic solutions, we place no restrictions on the location or number of neighboring quenchers, within the constraints of the lattice structure: each different state available to a fluorophore is weighted by its probability of occurring.

The independent-site model requires the use of different values of M, the maximum number of neighbor sites that can contribute to quenching, in order to fit the data for both single-chain quenchers and double-chain quenchers. Figure 3 shows theoretical curves for the independent-site model, from which we see that the quenching profile is quite sensitive to the efficiency of quenching: for a given value of M, the calculated curve depends *only* on the efficiency of quenching. If indeed the phospholipid itself were an independent quenching unit, then the number of neighbors should be the *same* regardless of the presence of quenching moieties on one or both chains of the phospholipid, and only the efficiency of quenching should change. Applying this independent-site model to TOE, TMA-DPH, and DPH-PC, we find that $M =$ 6 or 7 for quenching by SpinPC, whereas $M = 9$ or 10 for quenching by di-SpinPC (see insets of Figures 6–8). This discrepancy is not apparent for bromine quenching of TOE, which is too inefficient to make any distinction between $N =$ 6 or 9 (curves not shown).

This observation of differential effects of single- and double-chain quenchers leads to the second part of our theory. We have changed the model from considering the entire phospholipid molecule as a quenching unit to a model in which the acyl chains are quenchers, corresponding with the physical reality of the acyl chain lattice. With a Monte Carlo algorithm to ennumerate the distribution of acyl chains around the fluorophores, Figure 4 shows how the correlations of the sister chains of phospholipids, resulting in dependence of acyl site occupancy, affect the calculated fluorescence for single and double quenchers that have the same fluorescence in a membrane composed entirely of quenching phospholipid. With the dependent-site model, both the single- and double-chain quenchers are less efficient at every mole fraction of quencher in comparison to the independent-site model (dotted lines in Figure 4). This result may seem unexpected in the case of the double-chain quencher. However, we point out that the Monte Carlo ennumeration also accounts for the correlations of the unlabeled phospholipid chains, and for all mole fractions of quenching lipid, this effect decreases the total number of quenching chains around a fluorophore relative to independent quenchers. For the single-chain quencher, the effects of unlabeled chains on quencher occupancy are even more pronounced.

By use of the dependent-site Monte Carlo distributions for $M = 6$, 12, and 18 neighbor acyl sites, quenching curves were fit to the fluorescence data shown in Figures 5–8. For all the fluorophores quenched by SpinPC and di-SpinPC, the data consistently lie between $M = 18$ and $M = 12$, with a shift from 18 to 12 as the mole fraction of quencher increases. The same behavior is seen with both the single- and double-chain quenchers. The quenching of TOE by BrPC compared with di-BrPC is also consistent with the SpinPC vs di-SpinPC results, but the lower efficiency of quenching yields theoretical curves that are too closely spaced to distinguish between $M = 18$ and $M = 12$. However, M is greater than 6 (see Figure 5). Thus, in contrast to the independent-site model, the dependent-site model describes consistent quenching behavior for all the fluorophores, all efficiencies of quenching, and both the single and the double quenchers.

M is an operational parameter, which could, in principle, be dependent on the lifetime of the fluorophore, the mutual diffusion coefficient of the fluorophore and the phospholipid, and the structure of the lattice. In our model, we consider M to depend only on the lattice structure with no phospholipid exchange expected during the lifetime of the fluorophores. We found that with $M = 6$, i.e., quenching from only nearest

neighbors in a hexagonal lattice of acyl chains, none of the fluorophore–quencher pairs examined fit the data: M is always greater than 6, implying contributions from other neighbor shells. Given a fluorophore–quencher interaction distance of ~10 Å (see above), contributions would be expected from sites that are spaced ~5 Å from the 6 nearest neighbors (i.e., the next shell). The rates of quenching in neighbor shells might be expected to decrease with distance from the fluorophore. Implicit in our derivation, however, is an *average* k_q assigned to every lattice position occupied by a quencher, where k_q is related to M and F_M with eq 3.

Although a central feature of our model is that the *distribution of quenchers is static*, we speculate that the details of the quenching process must have dynamic contributions (e.g., rotational diffusion, chain "wobbling excursions", trans–gauche isomerizations, etc.). Such relative motions could allow quenching groups to move closer to the fluorophore during its fluorescence lifetime. In addition, since translational diffusion is negligible during the fluorescence lifetime, a "caging" of the quencher neighboring a fluorophore could enhance the dynamic interactions leading to quenching (Gösele et al., 1979).

The quenching of DPH-PC (Figure 8) is nearly indistinguishable from that of TMA-DPH (Figure 7). Although the permanent occupancy of a potential quenching site by the unlabeled sister chain of DPH-PC must result in a decrease in M by one site, for larger values of M (e.g., for M greater than ~12), the shape of the quenching curve hardly changes for $M \pm 1$.

The shift from $M = 18$ to $M = 12$ as the mole fraction of spin-labeled lipid increases indicates a deficiency in our model that might have several possible origins. The shift could arise from changes in k_q or M that must depend in some way on the concentration of quencher. We find that two complete nearest-neighbor shells ($M = 18$) with an average k_q assigned to all sites gives a good fit at low ($\chi < 0.1$) and high ($\chi > 0.6$) mole fractions of quencher for all fluorophores and efficient (nitroxide) quenchers. If the observed shift occurring in the interval $0.1 < \chi < 0.6$ were solely the result of a decrease in the chain quenching rate constant, k_q, as a function of concentration, then there would be no reason to expect that the rate would *increase* again at higher concentrations, as would be required to satisfy eq 3. A more likely explanation for the shift from $M = 18$ to 12 is based on the EPR observations. The EPR spectrum of the dilute di-SpinPC compared to that of SpinPC (Figure 2) suggests that the extent and/or rate of motion are(is) reduced when two labels neighbor each other, as judged by the increased hyperfine splitting (Freed, 1976). The possible steric hindrance inferred from the EPR spectrum of the di-SpinPC would translate to a new form of site dependence: steric inhibition of neighboring site occupancy, which is tantamount to a reduction in M. At high mole fractions of quencher, the steric effect would disappear because all the phospholipids would be identical; that is, the fluorescence quenching curve converges back to the theoretical line that was calculated without consideration of steric effects. To crudely approximate the steric exclusion effect of adjacent quencher groups, we have used a particular form of a Monte Carlo distribution for $M = 12$, calculated by not counting alternate sites in the ennumeration of the second nearest-neighbor shell: in effect, sites adjacent to a quencher chain were considered exclusively to prefer an unlabeled chain. The true functional form of steric exclusion is, of course, unknown, but it would result in a skewed probability distribution. A simple representation would be a site occupancy equilibrium perturbed by quencher–quencher interactions, which is another form of site dependence.

Table II: Quenching Rate Constants, k_q, for Quencher–Fluorophore Pairs

fluorophore/quencher	F_M[a]	k_q[b]
TOE/bromine	0.17	9.0×10^7
TOE/nitroxide	0.016	1.2×10^9
TMA-DPH/nitroxide	0.0043	1.6×10^9
DPH-PC/nitroxide	0.0046	1.5×10^9

[a] Determined with double-chain quenchers. [b] Quenching rates are s^{-1} per quenching chain. Rates calculated from eq 4 by assuming $\tau_0 = 3$ ns for TOE; $\tau_0 = 8$ ns for both TMA-DPH and DPH-PC; $M = 18$; $F_0 = 1.0$.

We make a simple comparison of the estimated quenching rate per chain (Table II) to typical dynamic quenching rates observed in solution: a membrane composed of a doubly labeled nitroxide phosphatidylcholine, molecular mass 880 g/mol with a density of approximately 1.0 g/cm^3 (Huang, 1969) is approximately equivalent to a 2.3 M solution of quencher within the lipid. For the nitroxide quencher, the total quenching rate for 18 nearest neighbors is then $\sim 18 \times (1.5 \times 10^9)\ s^{-1}/2.3\ M = 1.2 \times 10^{10}\ M^{-1}\ s^{-1}$, which is comparable to diffusion-controlled bimolecular quenching rates in solution (Lakowicz & Weber, 1973). Bromine quenching of TOE is ~10 times less efficient than is quenching by nitroxides.

A lifetime distribution analysis, based on our quenching model, depends only on the observation that fluorophores in contact with quenchers do have a measurable fluorescence, which corresponds to a rate model of deactivation. Instrumental limitations will conceal very short lifetime components of a complex decay (Lakowicz et al., 1987b), and so one may argue that the theory of static quenching is simply an approximation brought about by detection problems: there might be no "dark complex" in many cases of static quenching, but rather only high quenching rates that reduce the fluorescence lifetime below measurable levels. Fluorescence lifetimes have typically been analyzed as one, or the sum of several, exponential decays (Lakowicz, 1983; Ware, 1983). Many fluorophores exhibit a single-exponential decay in isotropic solvents, but show decays best fit by two or more exponentials in membranes (Wolber & Hudson, 1981). Multiple lifetimes imply some form of heterogeneity (Beecham & Brand, 1985). Recent work has led to the appealing hypothesis that fluorescence lifetimes are perhaps best described by a distribution since no fluorophore environments are expected to be identical during the lifetime of the excited state (Alcala et al., 1987; Fiorni et al., 1987; Gryczysnki et al., 1988; James & Ware, 1986; Williams & Stubbs, 1988). The nature of that distribution and its precise description, whether continuous or discrete, have not been determined. Discrimination between the proposed models is crucially dependent on the precision of the data (James & Ware, 1986; Lakowicz et al., 1987a).

Our results from the fluorescence quenching theory predict a functional form for the lifetime distribution: each lifetime corresponds to a particular number of quenching neighbors, with amplitudes proportional to the probability of their occurrence. These lifetimes and amplitudes can be used in the exponential series method of James and Ware (James et al., 1987; James & Ware, 1986), which is a discrete approximation to a continuous distribution of decay times where the lifetimes are fixed and the amplitudes are varied for a best fit. The only requirement for testing our model is the stipulation that the fluorophore must show single-exponential behavior (or at least very narrow, unimodal, distributional width) in pure phospholipids.

Lifetime distributions were calculated from occupancy distributions by using eq 12 and the known lifetime of the fluorophore in the absence of quencher. Figure 9 shows a theoretical lifetime distribution for a single-chain quencher with $F_M = 0.5$ or, equivalently, a phospholipid with an acyl chain that reduces the quantum yield of the fluorophore by 50% when the probe is completely surrounded by that lipid. The set of data is fit with both Gaussian and Lorentzian *continuous* distributions to illustrate the striking similarity of our discrete model to commonly used continuous distributions (Alcala et al., 1987; Fiorni et al., 1987; Lakowicz et al., 1987a; Williams & Stubbs, 1988). Use of the continuous distributions has no theoretical basis—they are merely convenient functions chosen to minimize the number of adjustable parameters for data analysis (Lakowicz et al., 1987a). However, symmetrical distributions, if used, should be applied to the distribution of *rate constants* for nonradiative decay, not the lifetime distribution (James et al., 1987), because the transformation of decay rates to lifetimes with eq 12 will distort any underlying symmetry, if its exists (Figure 9).

Table I shows sets of discrete lifetime distributions that were generated from our dependent-site model (with $M = 18$), together with the parameters used to fit these discrete distributions with Gaussian or Lorentzian models. In this comparison of the discrete vs continuous models, the chi-square statistic for the continuous distribution fits actually has no meaning with respect to the likelihood of agreement between the continuous and discrete models. Rather, we present the fits in order to justify our speculation that good fits to fluorescence lifetime data using continuous distributions could actually have a proper physical origin in the discrete distributions of quenching rates predicted by our model. We point out that substantial distributional widths can occur even with low concentrations of a lipid that causes a large change in quantum yield. In addition to acyl chain heterogeneity, the phospholipid head group can also affect the quantum yield of the fluorophore. For example, TMA-DPH in POPS shows a 20% lower fluorescence than in POPC (data not shown). Our analysis is consistent with the results of Williams and Stubbs (1988), who found increased distributional widths of DPH lifetimes (using a continuous, Lorentzian distribution model), relative to lifetimes in POPC, by introducing acyl chain heterogeneity (egg PC), and both acyl chain and head-group heterogeneity (microsomal lipid).

Any assumption of environmental homogeneity for a fluorophore, i.e., a single-exponential lifetime, is an oversimplification even in a pure solvent: there will always be some heterogeneity in the microenvironment of each fluorophore and therefore a multiplicity of excited states. The resulting distribution of decay times may not be discernible if the fluorophore is not particularly sensitive to different environments, or if the lifetime is long enough that environmental averaging occurs, or if instrumental limitations prevent detection of minor components. Fluorescence quenchers amplify the effects of environmental heterogeneity. We find that our model, developed to explain steady-state fluorescence quenching results, yields a lifetime distribution analysis that has a quantitative basis.

Acknowledgments

We thank Erwin London for helpful discussions and Mary Reppy for comments on the manuscript.

References

Alcala, J. R., Gratton, E., & Prendergast, F. G. (1987) *Biophys. J. 51*, 587.

Atik, S. S., & Singer, L. A. (1978) *J. Am. Chem. Soc. 100*, 3234.

Beecham, J. M., & Brand, L. (1985) *Annu. Rev. Biochem. 54*, 43.

Berkhout, T. A., Rietveld, A., & de Kruijff, B. (1987) *Biochim. Biophys. Acta 897*, 1.

Bieri, V. G., & Wallach, D. F. H. (1975) *Biochim. Biophys. Acta 406*, 415.

Binder, K., & Heermann, D. W. (1988) *Monte Carlo Simulation in Statistical Physics: An Introduction*, 1st ed., Springer-Verlag, Berlin.

Blatt, E., & Sawyer, W. H. (1985) *Biochim. Biophys. Acta 822*, 43.

Bligh, E. G., & Dyer, W. J. (1959) *Can. J. Biochem. Physiol. 37*, 911.

Boss, W. F., Kelley, C. J., & Landsberger, F. R. (1975) *Anal. Biochem. 64*, 289.

Caffrey, M., & Feigenson, G. W. (1981) *Biochemistry 20*, 1949.

Chattopadhyay, A., & London, E. (1987) *Biochemistry 26*, 39.

Cundall, R. B., Johnson, I., Jones, M. W., & Thomas, E. W. (1979) *Chem. Phys. Lett. 64*, 39.

Dawidowicz, E. A., & Rothman, J. E. (1976) *Biochim. Biophys. Acta 455*, 621.

Devaux, P., & McConnell, H. M. (1972) *J. Am. Chem. Soc. 94*, 4475.

Dewey, T. G., & Hammes, G. G. (1980) *Biophys. J. 32*, 1023.

East, J. M., & Lee, A. G. (1982) *Biochemistry 21*, 4144.

Eastman, M. P., Kooser, R. G., Das, M. R., & Freed, J. H. (1969) *J. Chem. Phys. 51*, 2690.

Eftink, M. R., & Ghiron, C. A. (1976) *Biochemistry 15*, 672.

Estep, T. N., & Thompson, T. E. (1979) *Biophys. J. 26*, 195.

Feigenson, G. W. (1983) *Biochemistry 22*, 3106.

Fiorni, R., Valentino, M., Wang, S., Glaser, M., & Gratton, E. (1987) *Biochemistry 26*, 3864.

Fisher, M. E. (1961) *Phys. Rev. 124*, 1664.

Florine, K. I., & Feigenson, G. W. (1987) *Biochemistry 26*, 1757.

Florine-Casteel, K., & Feigenson, G. W. (1988) *Biochim. Biophys. Acta 941*, 102.

Freed, J. H. (1976) in *Spin Labeling: Theory and Applications* (Berliner, L. J., Ed.) Academic Press, New York.

Fung, B. K., & Styer, L. (1978) *Biochemistry 17*, 5241.

Galla, H. J., Hartmann, W., Theilen, U., & Sackmann, E. (1979) *J. Membr. Biol. 48*, 215.

Gösele, U., Klein, U. K. A., & Hauser, M. (1979) *Chem. Phys. Lett. 68*, 291.

Green, J. A., Singer, L. A., & Parks, J. H. (1973) *J. Chem. Phys. 58*, 2690.

Gryczynski, I., Wiczk, W., Johnson, M. L., & Lakowicz, J. R. (1988) *Biophys. Chem. 32*, 173.

Haigh, E. A., Thulborn, K. R., & Sawyer, W. H. (1979) *Biochemistry 18*, 3525.

Haughland, R. P. (1989) *Handbook of Fluorescence Probes and Research Chemicals*, Molecular Probes, Inc., Eugene, OR.

Huang, C.-h. (1969) *Biochemistry 8*, 344.

Huang, N.-n., Florine-Casteel, K., Feigenson, G. W., & Spink, C. (1988) *Biochim. Biophys. Acta 939*, 124.

Jain, M. K., Rogers, J., Simpson, L., & Gierasch, L. M. (1985) *Biochim. Biophys. Acta 816*, 153.

James, D. R., & Ware, W. R. (1986) *Chem. Phys. Lett. 126*, 7.
James, D. R., Turnbull, J. R., Wagner, B. D., Ware, W. R., & Petersen, N. O. (1987) *Biochemistry 26*, 6272.
James, D. R., & Ware, W. R. (1986) *Chem. Phys. Lett. 126*, 7.
Janiak, M. J., Small, D. M., & Shipley, G. G. (1976) *Biochemistry 15*, 4575.
Janiak, M. J., Small, D. M., & Shipley, G. G. (1979) *J. Biol. Chem. 254*, 6068.
Jovin, T. M., & Vaz, L. C. (1989) *Methods Enzymol. 172*, 471.
Kates, M. (1986) *Techniques of Lipidology: Isolation, Analysis and Identification of Lipids*, 2nd ed., Elsevier, Amsterdam.
Kingsley, P. B., & Feigenson, G. W. (1979) *Chem. Phys. Lipids 24*, 135.
Lakowicz, J. R. (1983) *Principles of Fluorescence Spectroscopy*, Plenum Press, New York.
Lakowicz, J. R., & Weber, G. (1973) *Biochemistry 12*, 4161.
Lakowicz, J. R., Cherek, H., Gryczynski, I., Joshi, N., & Johnson, M. (1987a) *Biophys. Chem. 28*, 35.
Lakowicz, J. R., Johnson, M. L., Gryczynski, I., Joshi, N., & Laczko, G. (1987b) *J. Phys. Chem. 91*, 3277.
Lammers, J. G., Liefkens, T. J., Bus, J., & van der Meer, J. (1978) *Chem. Phys. Lipids 22*, 293.
Lehrer, S. S. (1971) *Biochemistry 10*, 3254.
Lentz, B. R., Barenholz, Y., & Thompson, T. E. (1976) *Biochemistry 15*, 4529.
Leto, T. L., Roseman, M. A., & Holloway, P. W. (1980) *Biochemistry 19*, 1911.
London, E. (1980) Ph.D Thesis, Cornell University.
London, E., & Feigenson, G. W. (1978) *FEBS Lett. 96*, 51.
London, E., & Feigenson, G. W. (1981a) *Biochemistry 20*, 1932.
London, E., & Feigenson, G. W. (1981b) *Biochemistry 20*, 1939.
London, E., & Feigenson, G. W. (1981c) *Biochim. Biophys. Acta 649*, 89.
Luzzati, V. (1968) in *Biological Membranes* (Chapman, D., Ed.) pp 71–123, Academic Press, London.
Markello, T., Zlotnick, A., Everett, J., Tennyson, J., & Holloway, P. W. (1985) *Biochemistry 24*, 2895.
Marsh, D. (1981) in *Membrane Spectroscopy* (Grell, E., Ed.) pp 51–142, Springer-Verlag, Berlin.
Medinger, T., & Wilkinson, F. (1965) *Trans. Faraday Soc. 61*, 620.
Mulders, F., van Langen, H., van Ginkel, G., & Levine, Y. K. (1986) *Biochim. Biophys. Acta 859*, 209.
Ohta, S., Shimaboyashi, A., & Aoho, M. (1982) *Synthesis* 833.
Parente, R. A., & Lentz, B. R. (1986) *Biochemistry 25*, 1021.
Prendergast, F. G., Haugland, R. P., & Callahan, P. J. (1981) *Biochemistry 20*, 7333.
Press, W. H., Flannery, B. P., Teukolsky, S. A., & Vetterling, W. T. (1986) *Numerical Recipes: The Art of Scientific Computing*, Cambridge Univeristy Press, Cambridge, U.K.
Reinert, J. C., Lowry, R. R., & Wickman, H. H. (1978) *Lipids 13*, 85.
Ruocco, M. J., & Shipley, G. G. (1982) *Biochim. Biophys. Acta 691*, 309.
Sklar, L. A., Miljanich, G. P., & Dratz, E. A. (1979) *Biochemistry 19*, 1707.
Snyder, B., & Freire, E. (1982) *Biophys. J. 40*, 137.
Spink, C. H., Yeager, M. D., & Feigenson, G. W. (1990) *Biochim. Biophys. Acta* (in press).
Staab, H. A. (1962) *Angew. Chem., Int. Ed. Engl. 1*, 351.
Straume, M., & Litman, B. J. (1987) *Biochemistry 26*, 5113.
Stubbs, C. D., Kouyama, T., Kinosita, K., & Ikegami, A. (1981) *Biochemistry 20*, 4257.
Thulborn, K. R., & Sawyer, W. H. (1978) *Biochim. Biophys. Acta 511*, 125.
Ware, W. R. (1983) in *Time-Resolved Fluorescence Spectroscopy in Biochemistry and Biology* (Cundall, R. B., & Dale, R. E., Eds.) pp 299–317, Plenum Press, New York.
Williams, B. W., & Stubbs, C. D. (1988) *Biochemistry 27*, 7994.
Wolber, P. K., & Hudson, B. S. (1979) *Biophys. J. 28*, 197.
Wolber, P. K., & Hudson, B. S. (1981) *Biochemistry 20*, 2800.
Yguerabide, J., & Foster, M. C. (1981) in *Membrane Spectroscopy* (Grell, E., Ed.) pp 199–269, Springer-Verlag, Berlin.